North Atlantic Multidecadal Climate Variability: An Investigation of Dominant Time Scales and Processes

LEELA M. FRANKCOMBE, ANNA VON DER HEYDT, AND HENK A. DIJKSTRA

Institute for Marine and Atmospheric Research Utrecht, Utrecht University, Utrecht, Netherlands

ABSTRACT

The issue of multidecadal variability in the North Atlantic has been an important topic of late. It is clear that there are multidecadal variations in several climate variables in the North Atlantic, such as sea surface temperature and sea level height. The details of this variability, in particular the dominant patterns and time scales, are confusing from both an observational as well as a theoretical point of view. After analyzing results from observational datasets and a 500-yr simulation of an Intergovernmental Panel on Climate Change (IPCC) Fourth Assessment Report (AR4) climate model, two dominant time scales (20–30 and 50–70 yr) of multidecadal variability in the North Atlantic are proposed. The 20–30-yr variability is characterized by the westward propagation of subsurface temperature anomalies. The hypothesis is that the 20–30-yr variability is caused by internal variability of the Atlantic Meridional Overturning Circulation (MOC) while the 50–70-yr variability is related to atmospheric forcing over the Atlantic Ocean and exchange processes between the Atlantic and Arctic Oceans.

1. Introduction

Analysis of multiple datasets of the Atlantic climate system has shown that many quantities show variations on a multidecadal time scale. The first analyses (Schlesinger and Ramankutty 1994; Kushnir 1994) were based on sea surface temperature (SST) and indicated variability on a time scale of 50–70 yr. Indeed, when a 10-yr running mean of North Atlantic SST anomalies is constructed, the Atlantic is found to have been coldest around 1920 and 1980, and relatively warm around 1950 as well as over the last decade (Enfield et al. 2001; Sutton and Hodson 2005). Although only a few cycles can be identified from the instrumental SST record, the variability is often referred to as the Atlantic multidecadal oscillation (AMO; Kerr 2000).

Water from the North Atlantic enters the Arctic Ocean through Fram Strait and the Barents Sea. The return flow of water from the Arctic occurs mainly via the East Greenland Current. This exchange forms an oceanic connection between the climates of the Arctic and the North Atlantic. Century-long records of sea ice extent in the Arctic display multidecadal variability (Venegas and Mysak 2000), which has been referred to as the low-frequency oscillation (LFO; Polyakov and Johnson 2000). This variability is strongest in the Kara Sea and decays toward the Canada Basin (Polyakov et al. 2003a). There are also multidecadal variations in sea ice transport through Fram Strait associated with the sea ice extent variability (Vinje et al. 2002).

The other connection between the North Atlantic and Arctic climates occurs through the atmosphere. The dominant atmospheric winter variability is the pattern of the North Atlantic Oscillation (NAO), with its Arctic extension, the Northern Annular Mode (NAM; Thompson and Wallace 2001). Although it cannot be demonstrated that the NAO has any significant preferential frequency, the Atlantic westerlies were relatively weak in the period between 1940 and 1970, and relatively strong from 1980 to the present. NAO variations impose a relatively well-known tripolar SST anomaly on the North Atlantic Ocean on seasonal to interannual time scales (Eden and Jung 2001; Alvarez-Garcia et al. 2008), while the low-frequency response of the ocean to the NAO is more of a basin-wide single-sign pattern (Visbeck et al. 2003).

A mechanistic understanding of the phenomena of multidecadal variability is important for several reasons. There are strong indications that summer temperatures

Corresponding author address: Leela M. Frankcombe, Dept. of Physics and Astronomy, Institute for Marine and Atmospheric Research Utrecht, Utrecht University, Princetonplein 5, 3584 CC Utrecht, Netherlands.
E-mail: l.m.frankcombe@uu.nl

in western Europe and precipitation variations, in particular in the continental United States, are related to the AMO (Enfield et al. 2001; Sutton and Hodson 2005). Second, multidecadal variations may contribute to changes in global mean surface temperature and hence may alternately mask and enhance temperature and precipitation changes due to increasing levels of greenhouse gases (Zhang et al. 2007). Third, if there are preferred patterns of multidecadal variability, then these may play a significant role in climate predictability on these time scales (Griffies and Bryan 1997; Keenlyside et al. 2008). Finally, understanding this variability is an important component of any general theory of climate variability and climate change.

This study is motivated by the rather contradictory results that have appeared in studies with general circulation (climate) models (GCMs) of multidecadal variability in the North Atlantic climate system. A time scale of SST variability close to 25 yr has been found in several GCMs (Timmermann et al. 1998; Cheng et al. 2004; Dong and Sutton 2005). On the other hand, Jungclaus et al. (2005) and Vellinga and Wu (2004) found dominant Atlantic SST variability on time scales of 70 and 100 yr, respectively. A variety of mechanisms of the phenomena (Delworth et al. 1993; Vellinga and Wu 2004; Jungclaus et al. 2005; Knight et al. 2005) have been suggested based on GCM results. Some suggest that coupled ocean–atmosphere interaction (Timmermann et al. 1998) is necessary. Others explain it as a dynamical oceanic response to atmospheric low-frequency variability (Delworth and Greatbatch 2000). Finally, a central role for the Atlantic–Arctic connection has been suggested (Jungclaus et al. 2005), while others attribute a role to processes in the tropical Atlantic (Vellinga and Wu 2004; Knight et al. 2005).

In this paper, we analyze results from many observational datasets and from a long simulation of version 2.1 of the Geophysical Fluid Dynamics Laboratory's Coupled Model (CM2.1) to provide a more detailed picture of North Atlantic multidecadal variability and the dominant processes involved. Our study provides support to the hypothesis that there are two dominant time scales of multidecadal variability in the North Atlantic climate system: a 20–30- and a 50–70-yr variability. We argue that the 20–30-yr variability is caused by internal variability of the Atlantic Meridional Overturning Circulation (MOC), while the longer 50–70-yr variability is related to low-frequency atmospheric forcing and Arctic–Atlantic exchange processes.

In section 2 we (re)analyze both oceanic, atmospheric, and cryospheric observations as well as a control simulation of the GFDL CM2.1 with a focus on the dominant time scales of the multidecadal variability in the North
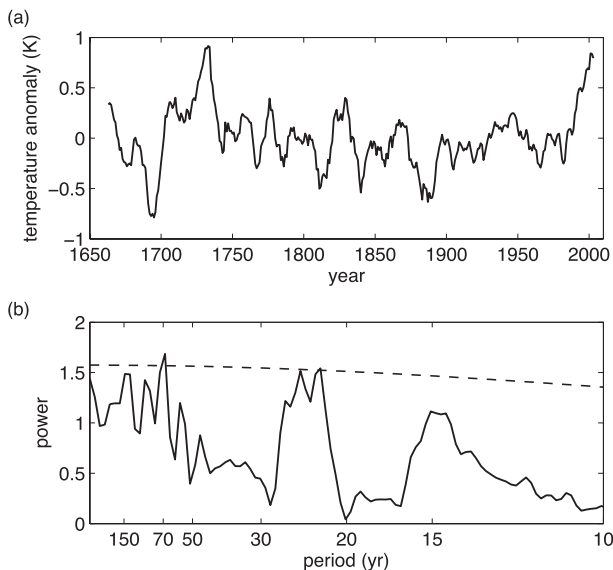

FIG. 1. (a) Time series (linearly detrended and smoothed with a 10-yr running mean filter) and (b) SSA spectrum of the (unsmoothed) CET record. The dashed curve is the 99% significance level using red noise as the null hypothesis.

Atlantic and Arctic Oceans. In section 3 we study the spatial patterns of variability by using Multichannel Singular Spectrum Analysis (M-SSA; Ghil et al. 2002), and in section 4 we discuss possible mechanisms for the 20–30- and 50–70-yr variability. Our main conclusions are presented and discussed in section 5.

2. Dominant multidecadal time scales

In this section, we consider the temporal signature of North Atlantic climate multidecadal variability using observations (section 2a) and GCM results (section 2b).

a. Observations

The fact that the North Atlantic SST observations used to define the AMO are at most 150 yr long gives rise to problems in detecting and understanding multidecadal variability. We can, however, also study variability in the North Atlantic Ocean by using land-based observations, since the basin-wide temperature anomalies that characterize the AMO affect the climate of the surrounding landmasses (Sutton and Hodson 2005).

There are only a few directly measured time series from which multidecadal variability can be reliably determined. One of these is the central England (CET) record, which dates back to the second half of the seventeenth century (Fig. 1a). The SSA spectrum (Ghil and Vautard 1991) of this time series (Fig. 1b) indicates that the dominant time scales of variability are in the 20–30-yr band (consistent with the analysis of this time series
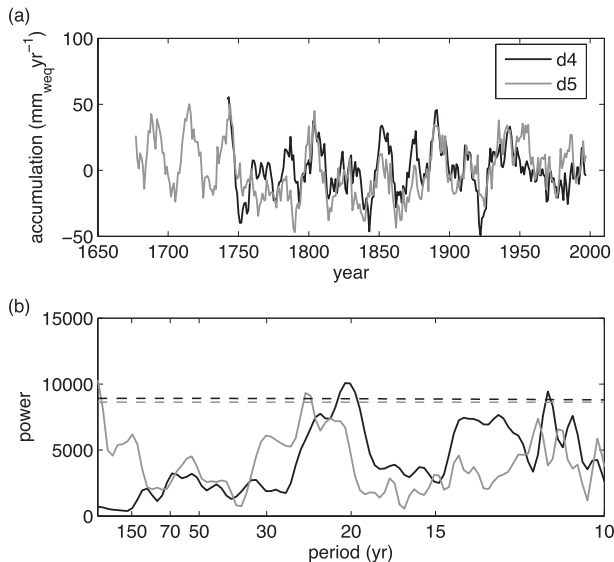
(a)

(b)

FIG. 2. (a) Time series (linearly detrended and smoothed with a 10-yr running mean filter) and (b) SSA spectra of the (unsmoothed) net snow accumulation rates (in mm of water equivalent per year) for two Greenland ice cores (Banta and McConnell 2007). The dashed curves are the 90% significance level.
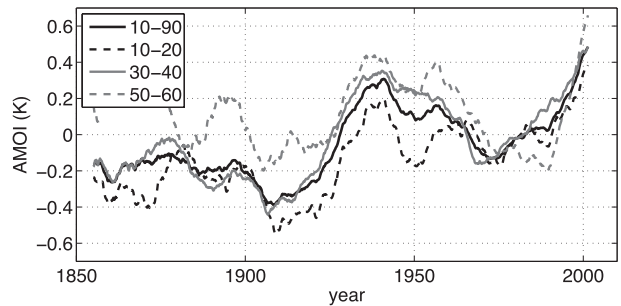

FIG. 3. Latitudinal band averages of temperature anomalies in the North Atlantic from the HadSST2 dataset. The solid black curve shows temperature anomalies averaged over the basin from 10° to 90°N, the dashed black curve shows anomalies averaged from 10° to 20°N, the solid gray curve from 30° to 40°N, and the dashed gray curve from 50° to 60°N. A 10-yr running mean filter has been applied to remove short time-scale variability.

presented in Plaut et al. 1995) and at approximately 70 yr. Both of these peaks are significant at the 99% level.

In the absence of other long instrumental time series, we turn to proxy records. Proxy data go back longer in time, but for these data an additional interpretation step is needed. Long series of net snow accumulation rates in central Greenland were obtained by Banta and McConnell (2007), and the time series and SSA spectra of the two longest of their four records are shown in Fig. 2. Both cores show variability at periods of 20–30 yr that is significant at the 90% level.

So why is it that the CET and Greenland ice cores show a dominant 20–30-yr variability while the basin-wide SST variability is suggested to have a dominant 50–70-yr variability (Schlesinger and Ramankutty 1994; Enfield et al. 2001)? To explain this we consider so-called latitudinal AMO indices, where the 10-yr running mean of the North Atlantic SST anomaly in 10° latitude bands is determined (Fig. 3) using SSTs from version 2 of the Hadley Centre Sea Surface Temperature (HadSST2) dataset (Rayner et al. 2006). Before about 1900, the variability at low latitudes appears to be out of phase with the variability at midlatitudes, so that the basin-wide-averaged variability (solid black curve in Fig. 3) is very small. This may also be due to the scarcity of data during this period. After 1900 the variability is much more coherent over latitude, with the cooler period around 1950 being much more pronounced at lower latitudes than at higher latitudes. The 20–30-yr component is dominant in each

individual latitudinal band, but although it remains visible in the basin-wide AMO index (AMOI), it appears to be overwhelmed by the 50–70-yr component. Further signatures of the 20–30-yr variability were found from the analysis of subsurface temperature (XBT) data in Frankcombe et al. (2008). Although there are only subsurface data from 1960 to 2000, it was suggested that the dominant period of variability is 20–30 yr. In Frankcombe and Dijkstra (2009), it is shown that tide gauge data around the North Atlantic also support the notion of a dominant time scale of 20–30 yr.

Apart from temperature (and salinity) anomalies in the North Atlantic Ocean, there are many other signatures of multidecadal variability in the North Atlantic climate system. In the Arctic, sea ice extent, the temperature of the Atlantic core water, and the atmospheric surface temperature all vary on multidecadal time scales (Venegas and Mysak 2000; Polyakov et al. 2003a,b, 2004; Divine and Dick 2006), with indications of a 50–70-yr period. In addition, there are the decadal-scale appearances of the Great Salinity Anomalies (GSAs) in the North Atlantic, of which several are thought to be connected to large sea ice exports out of the Arctic (Belkin et al. 1998). This makes the Arctic a likely candidate for affecting variability in the North Atlantic on the time scales of interest.

It is clear that variability in the North Atlantic Ocean propagates toward the Arctic through Fram Strait as well as along the Norwegian coast into the Barents Sea. Long time series of observations of sea ice extent in four Arctic seas are available and are plotted with the AMOI in Fig. 4a. As has already been shown by Polyakov et al. (2004), there is substantial multidecadal variability in sea ice extent, and correlations with the AMO index (significant at the 95% level in the Kara Sea; see Fig. 4b)

(a)

Sea ice extent anomalies and AMOI

(b)

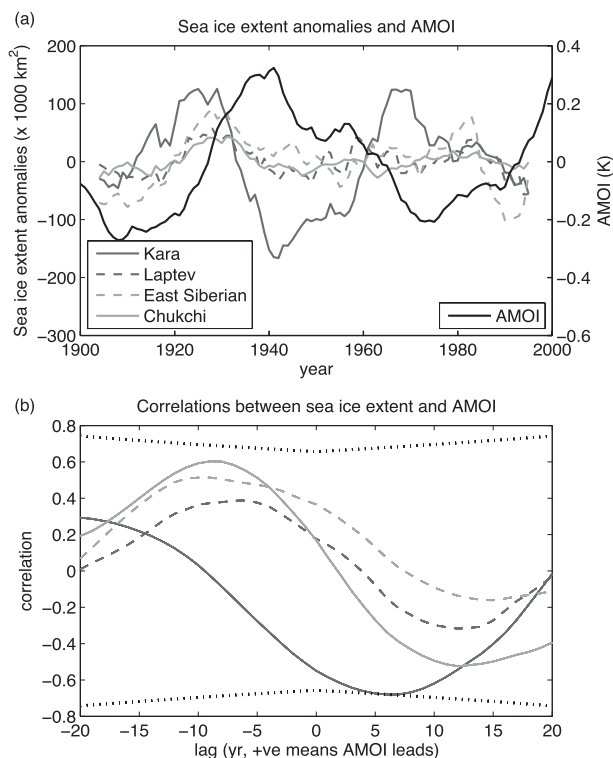Correlations between sea ice extent and AMOI

FIG. 4. (a) Observations of sea ice extent (smoothed with a 10-yr running mean filter) in four Arctic seas (from Polyakov et al. 2003a) along with the basin-wide AMOI (10°–90°N) and (b) correlations between each of them and the AMOI. The dotted line represents the 95% confidence interval.
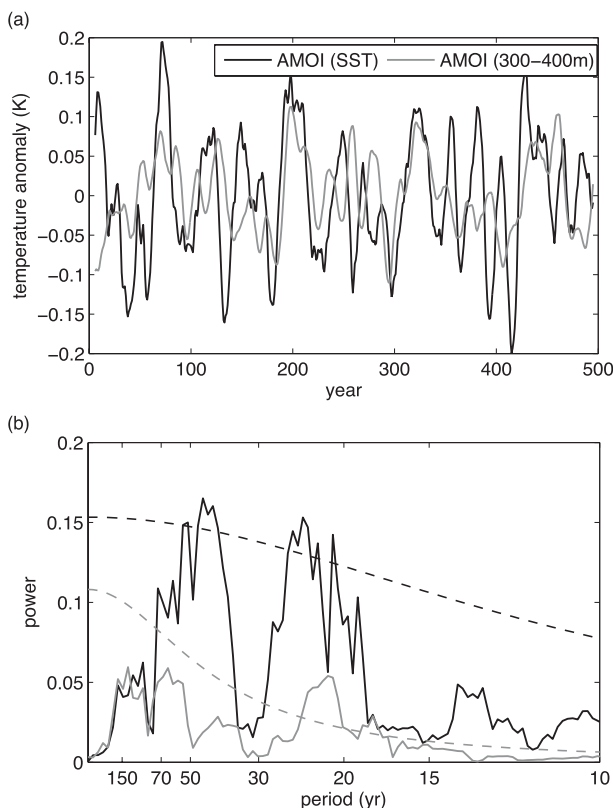

(a)

(b)

FIG. 5. (a) Time series (linearly detrended and smoothed with a 10-yr running mean filter) and (b) SSA spectra of two (unsmoothed) AMOIs (black, surface; gray, subsurface) of the last 500 yr of the CM2.1 control simulation (Zhang 2008). The dashed curves show the 99% significance levels.

show that a high AMO index precedes a minimum in sea ice extent. This is consistent with the propagation of warm Atlantic water into the Arctic causing a decrease in sea ice.

From the observations it is clear that, in addition to the previously described 50–70-yr variability found in the North Atlantic and Arctic, a dominant time scale of 20–30 yr may be found in SST over the North Atlantic as well as in temperatures in central England and net snow accumulation rates in Greenland.

b. GCM results

Several models from the Coupled Model Intercomparison Project (CMIP) suite (Stouffer et al. 2006) display clear multidecadal variability in the North Atlantic. We focus here only on the model control simulations, which have a time integration interval of longer than 500 yr. In particular, the recent analysis (Zhang 2008) of the 1000-yr control simulation of the GFDL CM2.1 model shows dominant variability on the 20–30-yr time scale (Fig. 2b in Zhang 2008). The first EOF shows a dipolar pattern in both SSH and subsurface temperature with strong positive anomalies south of Greenland and

negative anomalies in the Gulf Stream separation region. We analyzed the last 500 yr of this simulation (for which data were available) in more detail by looking at the variability in surface, as well as subsurface, temperatures. The AMO indices (North Atlantic between 10° and 80°N) for SST and for the 300–400-m-averaged subsurface temperature are plotted in Fig. 5a and their spectra in Fig. 5b. The basin-wide signal displays variability on both the 20–30- and 50–70-yr time scales, both at and below the surface. When the spectra of the AMO indices (surface and subsurface) are analyzed per latitudinal band (Fig. 6), one finds (similarly to in the observations) shorter periods at lower latitudes and in the subsurface and larger periods at midlatitudes and at the surface. Note that for every latitude, however, the 20–30-yr subsurface variability has significant energy.

The result from the GFDL CM2.1 model that there exist two dominant time scales of variability is also in accordance with some other GCMs in the CMIP suite. In a 1000-yr control simulation of the third climate configuration of the Met Office Unified Model (HadCM3), Dong and Sutton (2005) find variability in the Atlantic
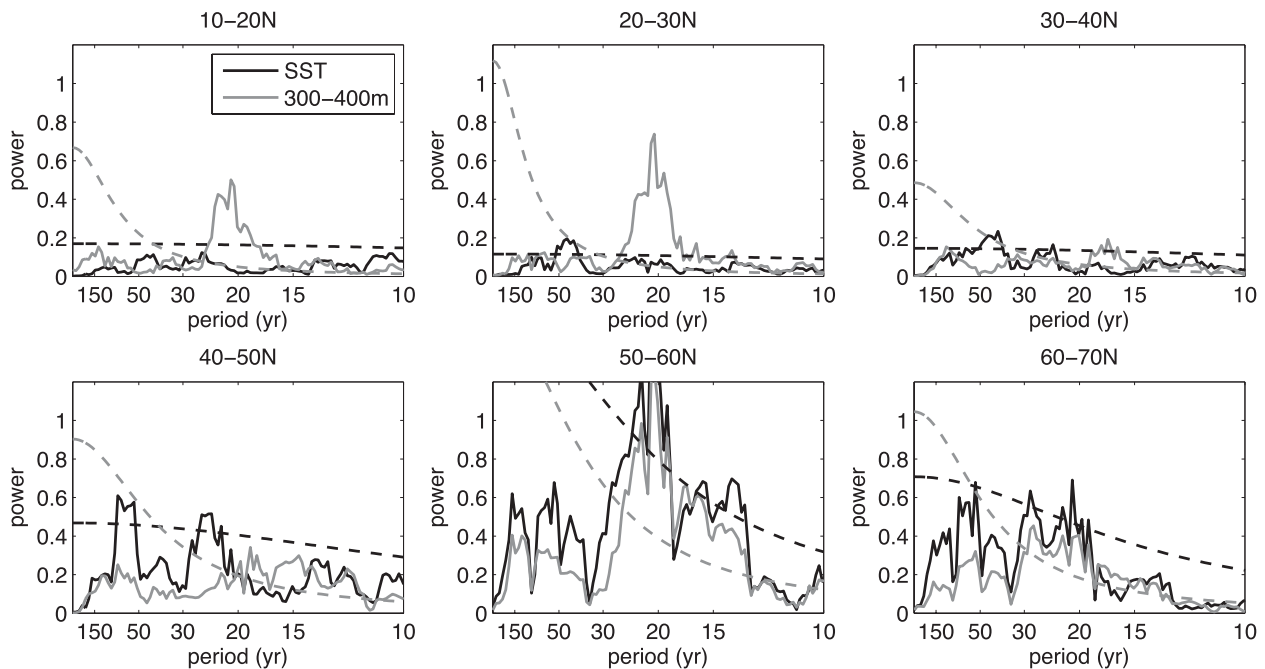
FIG. 6. Spectra of the latitudinal band anomalies of (unsmoothed) temperature in the GFDL CM2.1 control simulation (black, SST; gray, subsurface). The dashed curves show the 95% significance levels.

MOC with a dominant time scale of about 25 yr. There is also variability at the 50–70-yr band, but this is not significant [not even at the 90% level; see Fig. 2 in Dong and Sutton (2005)], although there is significant variability at the 100-yr time scale. Vellinga and Wu (2004) analyze this 100-yr variability in a 1600-yr control simulation of HadCM3. From the anomaly patterns of the model at this time scale, it is clear that there is no westward propagation and that the time scale is too long for their mechanism to be a plausible candidate for the 20–30-yr variability as found in the observations. The HadCM3 model simulation, however, also shows variability at the 20–30-yr time scale (Fig. 4 in Vellinga and Wu (2004)). Jungclaus et al. (2006) analyze a 500-yr control integration with the ECHAM5–Max Planck Institute Ocean Model (MPI-OM) and find pronounced multidecadal fluctuations in the Atlantic MOC and associated heat transport with a period of 70–80 yr. From a different simulation with the same model (Sterl et al. 2008), it appears that the dominant variability in the AMO index is in the 20–40-yr band. Variability on the longer time scale (50–80 yr) also exists but it is not significant at the 95% level (van Oldenborgh et al. 2009).

3. Dominant spatial patterns

Because of the relatively short observational time series (approximately 150 yr of SST and SLP), it is difficult to extract a dominant pattern of multidecadal variability with much confidence. Kaplan et al. (1997) and Delworth and Mann (2000) present a reconstruction of a signal with an approximately 50-yr period that shows a near-standing pattern in SST and SLP. The SST pattern is basin wide with the largest anomalies appearing south of Greenland.

In the GFDL CM2.1 model results, however, much more detail on the spatial patterns can be obtained. In the meridionally averaged Hovmöller diagrams at the surface (Fig. 7a), the dominant period appears to be 50–70 yr, while in the subsurface data (especially in the western part of the domain) the anomalies have larger amplitude and the shorter period appears to be dominant (Fig. 7b). The difference between the dominant time scales of variability at different depths is most clearly seen in Fig. 7c, in which the upper part of the plot shows the basin-averaged temperature anomalies at various depths. The lower plot shows a Hovmöller diagram of time versus basin-averaged temperature anomalies down to a depth of 1000 m. The time scale of the variability is shortest in the subsurface (near 200–300-m depth) and is longer both above and below this depth.

An M-SSA analysis was performed on the model results, focusing on the periods and horizontal patterns of temperature and salinity at the surface and at a depth of 400 m, both over the North Atlantic up to the Arctic Basin (with the domain 18.7°–90°N and 78°W–40°E) and over the Arctic alone (domain north of 70°N). The depth
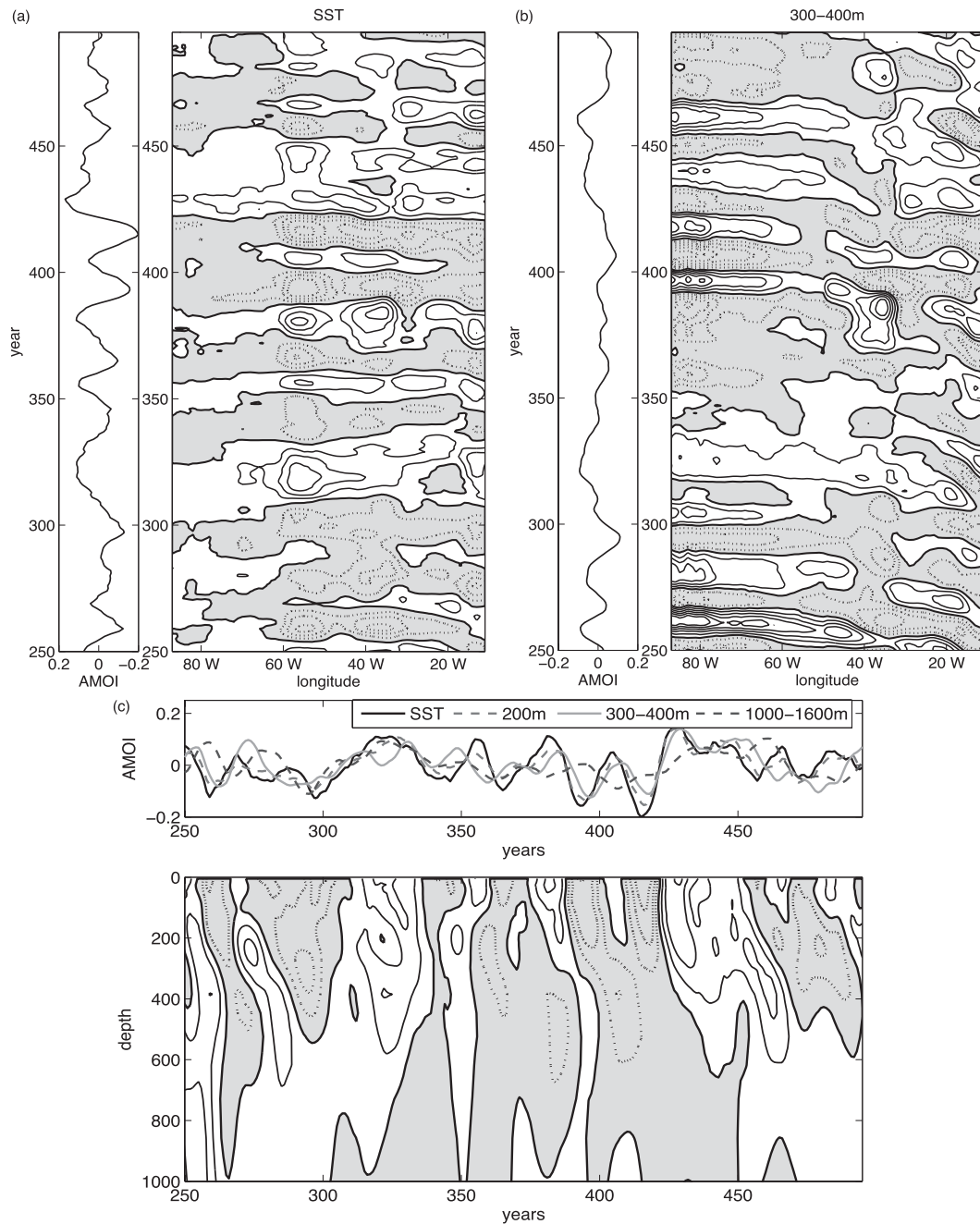
FIG. 7. (a) Basin-averaged AMOI (left) and a Hovmöller diagram of meridionally (10°–90°N) averaged SST anomalies (right) from the last 250 yr of the CM2.1 control simulation. (b) As in (a) but for the subsurface T'. (c) Basin-averaged T' at different depths (top) and a Hovmöller plot of basin-averaged T' vs depth (bottom). Data have been smoothed with a 10-yr running mean filter. Negative regions are shaded. The contour interval is 0.1 K in (a) and (b), and 0.05 K in (c).

of 400 m was chosen since that is the approximate depth of the layer of Atlantic water in the Arctic Ocean. A window length of 100 yr was used and the data were not smoothed beforehand. Two methods of estimating the lag covariance matrix were used [Vautard–Ghil (Vautard

et al. 1992) and reduced covariance], as well as two significance tests (Monte Carlo and chi squared). A peak was judged to be significant if it was above the 95% significance level in both tests using both estimation methods. The significant M-SSA modes are listed in Table 1 along

TABLE 1. Periods and variance of the significant M-SSA modes. The analysis was carried out over two domains—the North Atlantic (18.7°–90°N, 78°W–40°E) and the Arctic (north of 70°N)—for four variables: SST, sea surface salinity (SSS), T_{400}, and S_{400}. For each significant mode, the period and percent variance explained are listed, along with the figure number of the modes whose spatial patterns are plotted.

Domain	Quantity	Period (yr)	Variance (%)	Figure
North Atlantic	SST	20–30	7.4	Fig. 8
		~15	4.6	
	SSS	20–30	7.7	
	T_{400}	20–30	13.7	Fig. 9
		~15	6.6	
	S_{400}	20–30	15.7	
Arctic	SST	30–50	5.2	Fig. 10
		20–30	4.6	
	SSS			
	T_{400}	20–30	10.2	
	S_{400}	>50	35.4	Fig. 11
		30–70	18.4	
		30–50	13.6	
		30	9.5	Fig. 12
		20–30	4.2	

with the percentage of the variance that they explain and their periods (where the period was calculated using the spectra of the principal components of each mode). The analysis found, in general, that certain periods emerged repeatedly from the M-SSA analysis; the recurring peaks were at approximately 15, 20–30, 30–50, and 50–70 yr, and occasionally had a greater than 70-yr peak. However, not all of these peaks were found to be significant. When the domain included the North Atlantic, only the 20–30- and sometimes the 15-yr peaks were significant, while in the Arctic the longer periods also emerged above the red noise.

Figure 8 shows the leading pattern that results from the M-SSA analysis of SST anomalies in the GFDL CM2.1 control simulation. This oscillation has a period of 20–30 yr. Other very similar spatial patterns with periods of 30–50 and 50–70 yr also emerge, although they are not found to be significant. The temperature patterns at 400-m depth have their main region of variability farther south (Fig. 9), although the 20–30-yr period remains the same. As for SST, similar patterns are found for longer periods. The M-SSA modes of salinity at the surface and at a depth of 400 m over this domain show very similar periods and spatial patterns to the temperature modes.

M-SSA modes of temperature in the Arctic show that the dominant variability at both the surface and 400 m is in the Nordic Seas and the Atlantic section of the Arctic, as in Fig. 10. The temperature anomalies do not penetrate far into the Arctic proper, although some deeper anomalies do propagate along the continental shelf. Warm water from the North Atlantic can thus contribute to melting sea ice in the Arctic marginal seas, which is consistent with the observations of sea ice extent lagging the AMO index (shown in Fig. 4).

No significant oscillatory variability is found in the salinity at the surface in the Arctic Ocean. There is, however, significant variability in the salinity at 400-m depth on a range of time scales. The dominant period is 50–100 yr. This variability is concentrated in the Beaufort Sea but anomalies spread over the whole Arctic (Fig. 11). Coupling between the North Atlantic and the Arctic is seen in salinity at the same depth but on the shorter 20–30-yr time scale. Figure 12 shows how a salinity anomaly from the North Atlantic enters the Arctic and travels eastward around the basin. Anomalies propagating from the Arctic back to the North Atlantic would flow through Fram Strait and along the coast of Greenland and may provide a mechanism for the so-called Great Salinity Anomalies (Belkin et al. 1998).
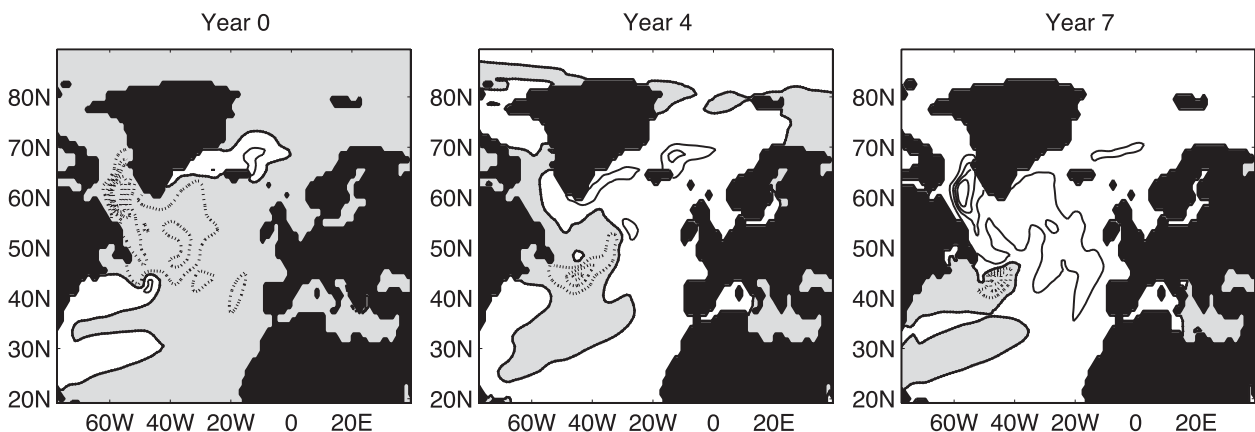

FIG. 8. Spatial pattern of the first M-SSA pair of North Atlantic SST, with a period of 20–30 yr, explaining 7.4% of the variance. The amplitude is arbitrary, negative regions are shaded, and the zero contour is set in boldface.
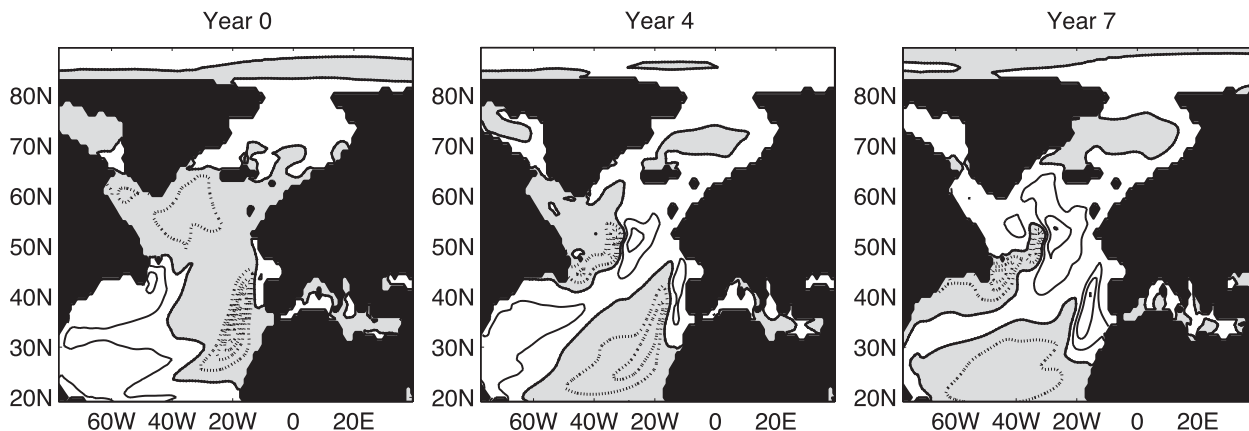
FIG. 9. Spatial pattern of the first M-SSA pair of temperature at 400 m T_{400}, with a period of 20–30 yr, explaining 13.7% of the variance.

Modes of atmospheric variability over the Arctic can be studied through an M-SSA analysis of modeled sea level pressure. The unfiltered time series shows variability only on shorter time scales (less than 20 yr), but if the data are filtered to allow periods of between 30 and 100 yr, then significant variability between 30 and 50 yr becomes apparent (not shown).

4. Physical mechanisms

From the analysis of available observations and control runs of the Intergovernmental Panel on Climate Change's (IPCC) Fourth Assessment Report (AR4) coupled models, it can be concluded that the 20–30-yr variability is present in both the observations and models, and that the subsurface temperature signal is associated with westward propagation. Another signal appears at the 50–70-yr time scale, and in addition variability at centennial scales (approximately100 yr) is found in models such as HadCM3. In section 4a, we discuss a possible mechanism for the 20–30-yr variability. This is followed by a section

where we propose several mechanisms to explain the 50–70-yr variability.

a. Physics of the 20–30-yr variability

The 20–30-yr variability can be understood in terms of the excited internal mode mechanism as developed from idealized models (te Raa and Dijkstra 2002; Frankcombe et al. 2009). Although this mechanism has already been presented in the literature a few times, we repeat it here as it is central to explaining the observed and modeled variability.

The westward propagation of subsurface anomalies is characteristic of the variations. This westward propagation is associated with Rossby-type dynamics but the background potential vorticity gradient is set by the background temperature gradient. In idealized (three-dimensional primitive equation) ocean models, the background meridional overturning circulation can become unstable due to growth of such a propagating and oscillatory perturbation (te Raa and Dijkstra 2002; Sévellec et al. 2009).
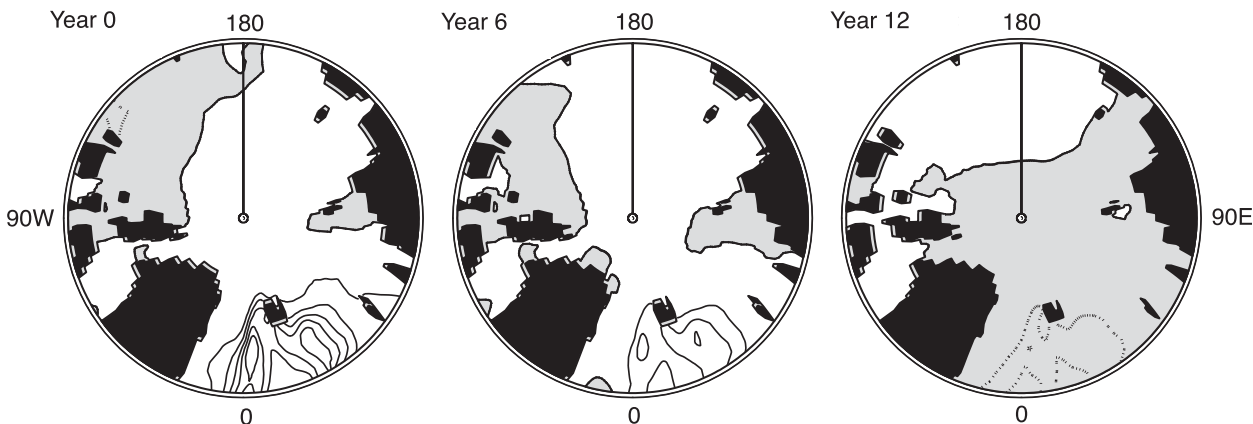

FIG. 10. Spatial pattern of the first M-SSA pair of SST over the Arctic with a period of 30–50 yr, explaining 5.2% of the variance.
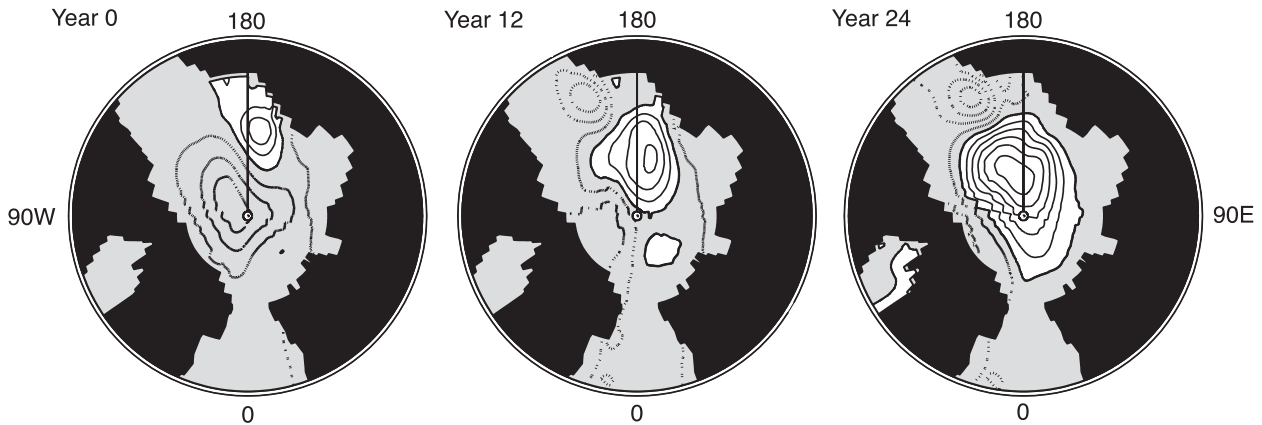
FIG. 11. Spatial pattern of the first M-SSA pair of salinity at 400-m depth S_{400} over the Arctic with a period longer than 50 yr. This pair explains 35.4% of the variance.

A slight generalization of this mechanism (compared to that in te Raa and Dijkstra 2002) is provided with help of Fig. 13. A warm anomaly in the north-central part of the basin causes a positive meridional perturbation temperature gradient, which induces—via the thermal wind balance—a negative zonal surface flow (Fig. 13a). The anomalous anticyclonic circulation around the warm anomaly causes southward (northward) advection of cold (warm) water to the east (west) of the anomaly, resulting in westward phase propagation of the warm anomaly. Due to this westward propagation, the zonal perturbation temperature gradient becomes negative, inducing a negative surface meridional flow (Fig. 13b). The resulting upwelling (downwelling) perturbations along the northern (southern) boundary cause a negative meridional perturbation temperature gradient, inducing a positive zonal surface flow, and the second half of the oscillation starts. The crucial elements in this oscillation mechanism are the phase difference between the zonal and meridional surface flow perturbations, and

the westward propagation of the temperature anomalies (te Raa and Dijkstra 2002). The time scale of the oscillation is set by the basin-crossing time of the anomalies. The presence of salinity does not essentially change this mechanism; density anomalies will take over the role of temperature anomalies in the description above (te Raa and Dijkstra 2003).

It was shown in Delworth and Greatbatch (2000) that while the variability is due to what is essentially an ocean-only mode, atmospheric noise is crucial to the excitation of the oscillations. Low-pass-filtered surface heat fluxes are most efficient at exciting the variations. Frankcombe et al. (2009) found that atmospheric noise is required to excite the oscillatory variability to sufficient amplitude since the meridional overturning is stable under realistic thermal damping by the atmosphere. The heat flux forcing associated with the low-frequency part of the NAO (pattern and amplitude) is beneficial for the excitation of the oceanic variability, as this forcing rectifies the background meridional overturning.
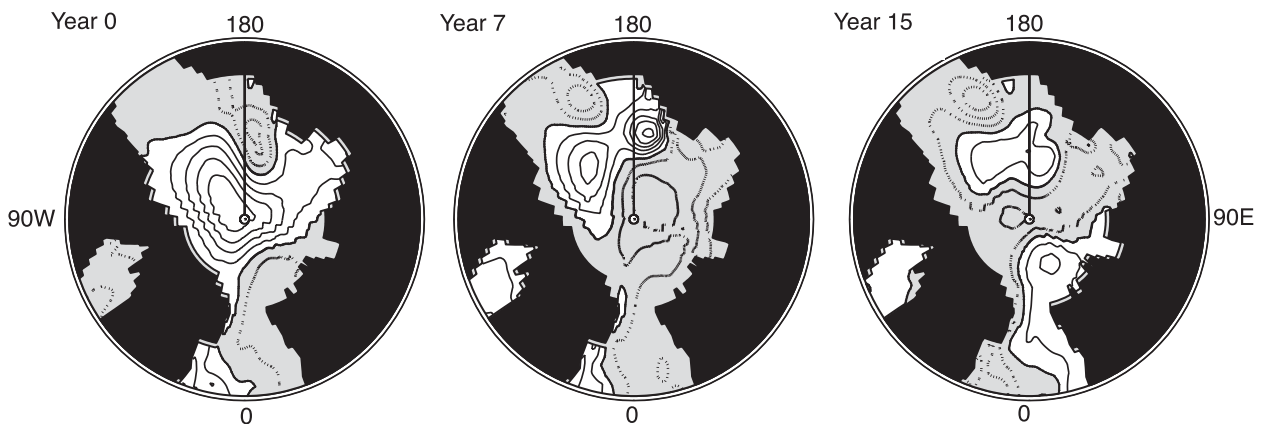

FIG. 12. Spatial pattern of the fourth M-SSA pair of S_{400} over the Arctic with a period of 30 yr, explaining 9.5% of the variance.
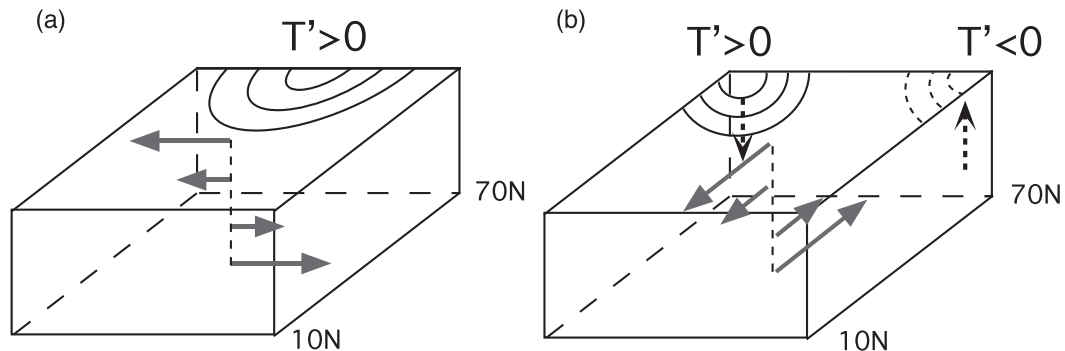
FIG. 13. Schematic diagram of the oscillation mechanism associated with the multidecadal mode caused by the westward propagation of T'. The phase difference between (a) and (b) is approximately a quarter period. See text and te Raa and Dijkstra (2002) for a further explanation.

The most convincing characteristic of this mechanism (i.e., the westward propagation of temperature anomalies) is indeed found in subsurface temperature observations (Frankcombe et al. 2008). In Fig. 3a of Frankcombe et al. (2008), which shows a Hovmöller plot of temperature anomalies, basin (10°–60°N) and vertically averaged over 300–400 m, westward propagation is easily identified. For example, the mid-Atlantic subsurface warming (at 60°W), which was at a maximum around 1978, started in the eastern part of the basin around 1970 and reached the western periphery around 1981. The phase differences between the zonal and meridional temperature differences show a maximum correlation around 5 yr, which leads, according to the mechanism above, to an estimate of the period of approximately 20 yr, consistent with the variability in the central England temperature record (Fig. 1). Phase differences between variability on the eastern and western boundaries of the North Atlantic are also found in sea level (Miller and Douglas 2007; Frankcombe and Dijkstra 2009) and can also be explained by westward-propagating anomalies with a time scale of 20–30 yr.

There is also clear westward propagation in the subsurface temperature field in the GFDL CM2.1 control simulation, as can be seen from Fig. 7b. The SST signal is much more stationary at the surface in Fig. 7a, which is also seen in the observations. This difference in propagation can be explained by the theory of te Raa and Dijkstra (2002), as the background zonal flow is a parameter in the propagation speed.

Results from other GCMs may be reconsidered in relation to this mechanism. Dong and Sutton (2005) found two significant peaks in the spectrum of MOC variability in HadCM3: one at approximately 25 yr and one at approximately 90 yr. The shorter-period variability was associated with variations in density in the northern

North Atlantic, with the lagged correlations between density and overturning strength consistent with the mechanism discussed here. Delworth et al. (1993) also found MOC variability lagging density variations, as well as the westward propagation of anomalies at the surface.

With this many indications of westward propagation and a mechanism based on clear physics independent of frictional parameterizations (i.e., only based on thermal wind), we tend to place a great deal of confidence in the hypothesis that the 20–30-yr variability can be attributed to an excited multidecadal internal ocean mode, as in Dijkstra et al. (2008). We are then left with the issue of explaining the 50–70-yr variability.

b. Possible causes of the 50–70-yr variability

Considering the results of the analyses above, the 50–70-yr variability has the following properties distinguishing it from the 20–30-yr variability:

(i) it is more pronounced at the surface than in the subsurface in the North Atlantic and
(ii) it is the dominant variability in the Arctic Ocean, where it seen most clearly in subsurface salinity.

There are several possibilities for the source of the longer-period variability:

(i) modulation of the 20–30-yr variability,
(ii) excitation by the atmosphere,
(iii) interaction between the North Atlantic and tropical Atlantic, and
(iv) interaction between the North Atlantic and Arctic.

Each of these will be discussed below.

One possibility is that the 50–70-yr variability is caused by the same processes as the 20–30-yr variability. In idealized models, where an internal ocean mode is excited by atmospheric noise, the spectrum shows a broad peak at

multidecadal frequencies (see, e.g., Fig. 6b in Frankcombe et al. 2009). This means that both the 20–30- and 50–70-yr periods could be encompassed by the same spectral peak. However, Fig. 5 shows that the spectra of temperature variability in the North Atlantic seem to have distinct peaks at 20–30, 30–50, and 50–70 yr; thus, it seems that the variability has a preference for particular periods rather than being purely red (Hasselmann 1976). This could be caused by a series of weak oscillations followed by a particularly strong anomaly, making the period of the oscillation appear longer than the underlying 20–30 yr. This hypothesis is borne out by the M-SSA analysis of temperature and salinity in the North Atlantic in the GFDL CM2.1 control run, which finds oscillatory M-SSA pairs at the various frequencies that have very similar spatial patterns, but only the pairs showing variability at approximately 30 yr are significant.

A second possibility is that the 50–70-yr variability is forced by the atmosphere, in particular through multi-decadal variability of the North Atlantic Oscillation. This mechanism was considered in the study of Eden and Jung (2001), where an eddy-permitting ocean GCM was forced by heat, freshwater, and momentum anomalies of multi-decadal NAO variability. Although it was found that direct forcing by the NAO heat flux anomalies cannot explain the SST cooling during the 1970s, for example, it was shown that a lagged response of the Atlantic MOC to the forcing can explain this pattern of behavior. Clearly, the variability in Eden and Jung (2001) is on a much larger time scale than the 20–30-yr variability (e.g., their Fig. 3) and so the NAO forcing combined with a lagged MOC response cannot explain this shorter time-scale variability. Eden and Jung (2001) also show that the variability is mainly temperature controlled (i.e., salinity is not essential for its existence). Note that if the atmospheric forcing mechanism above describes the primary processes of the 50–70-yr variability, we would expect variability in the MOC on both the (internal) 20–30- and the (forced) 50–70-yr time scales.

A third possibility for the source of the 50–70-yr variability is modulation of the 20–30-yr variability by a tropical connection. Vellinga and Wu (2004) found that centennial fluctuations in the strength of the meridional overturning in HadCM3 were caused by processes in the tropics, with the period set by the travel time of the salinity anomalies from their generation region near the equator to the convection region in the subpolar North Atlantic. This process, however, is on a time scale too long to cause variability on the 50–70-yr time scale.

Hawkins and Sutton (2007) showed three-dimensional patterns of propagation of temperature and salinity anomalies in HadCM3 and found that salinity anomalies in the Arctic may also play an important role in the variability in that model, although in their case the variability was also on a centennial rather than multidecadal time scale.

This brings us to the final possible mechanism that arises through the interaction of the Atlantic with the Arctic, which appears to be a mechanism where salinity plays a crucial role. There is inflow of Atlantic water into the Arctic, which is a source of multidecadal variability of sea ice as shown by Polyakov et al. (2004). However, the signal quickly dissipates along the mean Arctic sub-surface circulation. The strong and significant subsurface salinity variability in the Arctic (as found by the M-SSA analysis) hence indicates that the Arctic has internal variability on 50–70-yr time scales. This variability may be associated with the LFO, as suggested by Polyakov et al. (2004), and possibly also to the GSAs. The LFO mechanism has an atmospheric component and requires feedback from the atmosphere to control the inflow of Atlantic water into the Arctic. This would entail variability in the atmosphere over the Arctic being on the same time scale as the Arctic variability. An M-SSA analysis of sea level pressure over the Arctic does indeed find long-period variability, but the only significant periods are between 30 and 50 yr rather than between 50 and 70 yr. We must also consider that the major variability in the Arctic in this model is in salinity rather than temperature, and below the surface rather than at the surface, so that variability in the Arctic atmosphere could very well be driven by something other than variability in the Arctic Ocean. While the ocean–atmosphere mechanism of the LFO cannot be discounted, it appears more likely, in this model, that variability in the Arctic atmosphere is driven by SSTs in the North Atlantic, inheriting the time scale from there, while variability in the Arctic Ocean could be generated internally and thus has its own time scale.

The involvement of the Arctic–Atlantic exchange is supported by GCM results where such a mechanism has been suggested to explain multidecadal variability. For example, Jungclaus et al. (2005) found that in the ECHAM5–MPI-OM model the overturning strength was affected by density anomalies generated in the Arctic and the subsequent oscillations had a period of 70–80 yr. A similar mechanism was suggested by Delworth et al. (1997) to explain 40–80-yr oscillations in the GFDL model. The Arctic exchange mechanism would be most visible at high latitudes and at the surface of the Atlantic Ocean, while one would not see strong subsurface signals, which is consistent with the distinguishing properties of the 50–70-yr variability discussed above. The role of the GSAs and subsequent changes in the Atlantic MOC is not clear: results on how the MOC changes due to salinity anomalies appear to be very model dependent,

with Zhang and Vallis (2006) finding a strong response but Haak et al. (2003) indicating hardly any.

5. Summary and conclusions

In this paper an analysis of time scales and patterns of North Atlantic multidecadal variability was presented. Explaining this variability is a daunting task because of the lack of data and a multitude of possible processes that may be involved and that may not be limited to the North Atlantic itself. The main result of this paper is that there are indications from observations, as well as GCM results, for dominant variability at both 20–30- and 50–70-yr time scales.

The 20–30-yr variability is clearly visible in midlatitude subsurface temperature fields both in the observations and in the GCM simulations. M-SSA analysis of the GFDL CM2.1 output shows that the spatial subsurface patterns in the North Atlantic display westward propagation, consistent with the observations. As this propagation is a characteristic feature of the excited internal ocean mode mechanism, this mechanism is the best candidate to explain many of the features of the 20–30-yr variability.

The simplest explanation for the longer-period (50–70 yr) variability is a modulation of the shorter-period (20–30 yr) variability. This would lead to both periods being visible in the spectrum of MOC variability, but would not explain why the longer-period variability is most pronounced in high-latitude SST anomaly fields, nor the depth dependence of the time scale of basin-averaged temperature anomalies in the GFDL CM2.1 control simulation, as shown in Fig. 7c. M-SSA analysis of the GFDL CM2.1 model results suggests that the source of the 50–70-yr period variability is an oscillation seen in salinity at 400-m depth in the Arctic. Note that 400 m is the approximate depth of the layer of Atlantic water in the Arctic. While the low-frequency oscillation of Polyakov et al. (2004) is an attractive explanation for this variability, we can find no firm basis for it in the GFDL model results. An alternative is that the inflow from the Atlantic may be exciting an internal salinity mode in the Arctic Basin, which, in turn, feeds anomalies back into the North Atlantic on longer time scales. This then suggests that GSAs are coupled to the internal variability of the Arctic.

Finally, these results may start the discussion of what one really calls the AMO. As research has developed, it would probably be better to reserve the term AMO for the longer 50–70-yr variability while referring to the 20–30-yr variability as the Atlantic interdecadal oscillation (AIO). In this case the AMO index needs to be redefined. Measurements of SST remain the most accessible method for constructing an index, but the domains may be altered. Restricting the domain, as in Fig. 3, to a narrower latitudinal band (e.g., 50°–60°N) would suffice for an index for the interdecadal variability, while the multidecadal variability could be indexed by expanding the domain to include the Arctic. This would allow a distinction between the various time scales and patterns of variability.

REFERENCES

Alvarez-Garcia, F., M. Latif, and A. Biastoch, 2008: On multi-decadal and quasi-decadal North Atlantic variability. *J. Climate,* **21,** 3433–3452.

Banta, J. R., and J. R. McConnell, 2007: Annual accumulation over recent centuries at four sites in central Greenland. *J. Geophys. Res.,* **112,** D10114, doi:10.1029/2006JD007887.

Belkin, I. M., S. Levitus, J. I. Antonov, and S.-A. Malmberg, 1998: "Great Salinity Anomalies" in the North Atlantic *Prog. Oceanogr.,* **41,** 1–68.

Cheng, W., R. Bleck, and C. Rooth, 2004: Multi-decadal thermohaline variability in an ocean–atmosphere general circulation model. *Climate Dyn.,* **22,** 573–590.

Delworth, T. L., and R. J. Greatbatch, 2000: Multidecadal thermohaline circulation variability driven by atmospheric surface flux forcing. *J. Climate,* **13,** 1481–1495.

——, and M. E. Mann, 2000: Observed and simulated multidecadal variability in the Northern Hemisphere. *Climate Dyn.,* **16,** 661–676.

——, S. Manabe, and R. J. Stouffer, 1993: Interdecadal variations of the thermohaline circulation in a coupled ocean–atmosphere model. *J. Climate,* **6,** 1993–2011.

——, ——, and ——, 1997: Multidecadal climate variability in the Greenland Sea and surrounding regions: A coupled model simulation. *Geophys. Res. Lett.,* **24,** 257–260.

Dijkstra, H. A., L. M. Frankcombe, and A. von der Heydt, 2008: A stochastic dynamical systems view of the Atlantic multidecadal oscillation. *Philos. Trans. Roy. Soc.,* **366A** (1875), 2545–2560.

Divine, D. V., and C. Dick, 2006: Historical variability of sea ice edge position in the Nordic Seas. *J. Geophys. Res.,* **111,** C01001, doi:10.1029/2004JC002851.

Dong, B., and R. T. Sutton, 2005: Mechanism of interdecadal thermohaline circulation variability in a coupled ocean–atmosphere GCM. *J. Climate,* **18,** 1117–1135.

Eden, C., and T. Jung, 2001: North Atlantic interdecadal variability: Oceanic response to the North Atlantic Oscillation (1865–1997). *J. Climate,* **14,** 676–691.

Enfield, D. B., A. M. Mestas-Nuñez, and P. J. Trimble, 2001: The Atlantic multidecadal oscillation and its relation to rainfall and river flows in the continental U.S. *Geophys. Res. Lett.,* **28,** 2077–2080.

Frankcombe, L. M., and H. A. Dijkstra, 2009: Coherent multidecadal variability in North Atlantic sea level. *Geophys. Res. Lett.,* **36,** L15604, doi:10.1029/2009GL039455.

——, ——, and A. von der Heydt, 2008: Sub-surface signatures of the Atlantic multidecadal oscillation. *Geophys. Res. Lett.,* **35,** L19602, doi:10.1029/2008GL034989.

——, ——, and ——, 2009: Noise-induced multidecadal variability in the North Atlantic: Excitation of normal modes. *J. Phys. Oceanogr.,* **39,** 220–233.

Ghil, M., and R. Vautard, 1991: Interdecadal oscillations and the warming trend in global temperature time series. *Nature,* **350,** 324–327.

——, and Coauthors, 2002: Advanced spectral methods for climatic time series. *Rev. Geophys.,* **40,** 1003, doi:10.1029/2000RG000092.

Griffies, S. M., and K. Bryan, 1997: Predictability of North Atlantic multidecadal climate variability. *Science,* **275,** 181–184.

Haak, H., J. Jungclaus, U. Mikolajewicz, and M. Latif, 2003: Formation and propagation of great salinity anomalies. *Geophys. Res. Lett.,* **30,** 1473, doi:10.1029/2003GL017065.

Hasselmann, K., 1976: Stochastic climate models. Part I: Theory. *Tellus,* **28,** 473–485.

Hawkins, E., and R. T. Sutton, 2007: Variability of the Atlantic thermohaline circulation described by three-dimensional empirical orthogonal functions. *Climate Dyn.,* **29,** 745–762.

Jungclaus, J. H., H. Haak, M. Latif, and U. Mikolajewicz, 2005: Arctic–North Atlantic interactions and multidecadal variability of the meridional overturning circulation. *J. Climate,* **18,** 4013–4031.

——, N. Keenlyside, M. Botzet, H. Haak, J.-J. Luo, J. Marotzke, U. Mikolajewicz, and E. Roeckner, 2006: Ocean circulation and tropical variability in the coupled model ECHAM5/MPI-OM. *J. Climate,* **19,** 3952–3972.

Kaplan, A., Y. Kushnir, M. A. Cane, and M. B. Blumenthal, 1997: Reduced space optimal analysis for historical data sets: 136 yr of Atlantic sea surface temperatures. *J. Geophys. Res.,* **102** (C13), 27 835–27 860.

Keenlyside, N. S., M. Latif, J. Jungclaus, L. Kornblueh, and E. Roeckner, 2008: Advancing decadal-scale climate prediction in the North Atlantic sector. *Nature,* **453,** 84–88.

Kerr, R. A., 2000: A North Atlantic climate pacemaker for the centuries. *Science,* **288,** 1984–1986.

Knight, J. R., R. J. Allan, C. K. Folland, M. Vellinga, and M. E. Mann, 2005: A signature of persistent natural thermohaline circulation cycles in observed climate. *Geophys. Res. Lett.,* **32,** L20708, doi:10.1029/2005GL024233.

Kushnir, Y., 1994: Interdecadal variations in North Atlantic sea surface temperature and associated atmospheric conditions. *J. Climate,* **7,** 141–157.

Miller, L., and B. C. Douglas, 2007: Gyre-scale atmospheric pressure variations and their relation to 19th and 20th century sea level rise. *Geophys. Res. Lett.,* **34,** L16602, doi:10.1029/2007GL030862.

Plaut, G., M. Ghil, and R. Vautard, 1995: Interannual and interdecadal variability in 335 yr of central England temperatures. *Science,* **268,** 710–713.

Polyakov, I. V., and M. A. Johnson, 2000: Arctic decadal and interdecadal variability. *Geophys. Res. Lett.,* **27,** 4097–4100.

——, and Coauthors, 2003a: Long-term ice variability in Arctic marginal seas. *J. Climate,* **16,** 2078–2085.

——, D. Walsh, I. Dmitrenko, R. L. Colony, and L. A. Timokhov, 2003b: Arctic Ocean variability derived from historical observations. *Geophys. Res. Lett.,* **30,** 1298, doi:10.1029/2002GL016441.

——, and Coauthors, 2004: Variability of the intermediate Atlantic water of the Arctic Ocean over the last 100 yr. *J. Climate,* **17,** 4485–4497.

Rayner, N. A., P. Brohan, D. E. Parker, C. K. Folland, J. J. Kenndy, M. Vanicek, T. J. Ansell, and S. F. B. Tett, 2006: Improved analysis of changes and uncertainties in sea surface temperature measured in situ since the mid-ninteenth century: The HadSST2 dataset. *J. Climate,* **19,** 446–469.

Schlesinger, M. E., and N. Ramankutty, 1994: An oscillation in the global climate system of period 65–70 yr. *Nature,* **367,** 723–726.

Sévellec, F., T. Huck, M. Ben Jelloul, and J. Vialard, 2009: Non-normal multidecadal response of the thermohaline circulation induced by optimal surface salinity perturbations. *J. Phys. Oceanogr.,* **39,** 852–872.

Sterl, A., and Coauthors, 2008: When can we expect extremely high surface temperatures? *Geophys. Res. Lett.,* **35,** L14703, doi:10.1029/2008GL034071.

Stouffer, R. J., and Coauthors, 2006: Investigating the causes of the response of the thermohaline circulation to past and future climate changes. *J. Climate,* **19,** 1365–1387.

Sutton, R. T., and D. L. Hodson, 2005: Atlantic Ocean forcing of North American and European summer climate. *Science,* **309,** 115–118.

te Raa, L. A., and H. A. Dijkstra, 2002: Instability of the thermohaline ocean circulation on interdecadal timescales. *J. Phys. Oceanogr.,* **32,** 138–160.

——, and ——, 2003: Sensitivity of North Atlantic multidecadal variability to freshwater flux forcing. *J. Climate,* **16,** 2586–2601.

Thompson, D. W. J., and J. M. Wallace, 2001: Regional climate impacts of the Northern Hemisphere Annular Mode. *Science,* **293,** 85–89.

Timmermann, A., M. Latif, R. Voss, and A. Grötzner, 1998: Northern Hemisphere interdecadal variability: A coupled air–sea mode. *J. Climate,* **11,** 1906–1931.

van Oldenborgh, G. J., L. A. te Raa, H. A. Dijkstra, and S. Y. Philip, 2009: Frequency- or amplitude-dependent effects of the Atlantic meridional overturning on the tropical Pacific Ocean. *Ocean Sci.,* **5,** 293–301.

Vautard, R., P. Yiou, and M. Ghil, 1992: Singular-spectrum analysis: A toolkit for short, noisy chaotic signals. *Physica D,* **58,** 95–126.

Vellinga, M., and P. Wu, 2004: Low-latitude freshwater influence on centennial variability of the Atlantic thermohaline circulation. *J. Climate,* **17,** 4498–4511.

Venegas, S. A., and L. A. Mysak, 2000: Is there a dominant timescale of natural climate variability in the Arctic? *J. Climate,* **13,** 3412–3434.

Vinje, T., T. B. Loyning, and I. Polyakov, 2002: Effects of melting and freezing in the Greenland Sea. *Geophys. Res. Lett.,* **29,** 2129, doi:10.1029/2002GL015326.

Visbeck, M., E. P. Chassignet, R. G. Curry, T. L. Delworth, R. R. Dickson, and G. Krahmann, 2003: *The North Atlantic Oscillation: Climatic Significance and Environmental Impact.* Geophys. Monogr., Vol. 134, Amer. Geophys. Union, 279 pp.

Zhang, R., 2008: Coherent surface-subsurface fingerprint of the Atlantic meridional overturning circulation. *Geophys. Res. Lett.,* **35,** L20705, doi:10.1029/2008GL035463.

——, and G. K. Vallis, 2006: Impact of great salinity anomalies on the low-frequency variability of the North Atlantic climate. *J. Climate,* **19,** 470–482.

——, T. L. Delworth, and I. M. Held, 2007: Can the Atlantic Ocean drive the observed multidecadal variability in Northern Hemisphere mean temperature? *Geophys. Res. Lett.,* **34,** L02709, doi:10.1029/2006GL028683.